Emergency Restorability of Underground Engineering Environment after Disasters by Utilizing Prefabrication and Assembly Technology

Tong Qiu, Ph.D., S.M.ASCE[1]; Xiangsheng Chen, Ph.D.[2]; and Dong Su, Ph.D.[3]

Abstract: Urban development is promoting aboveground-underground city integration. Underground engineering and surrounding buildings and infrastructure form an underground engineering environment (UEE). In critical disasters, damage to the UEE not only causes chain damage to the surroundings but also aggravates urban resilience. Few studies have focused on UEE resilience and its disaster reduction. This study investigated the emergency restorability of the UEE to fill this research gap. First, we classified the restoration levels based on UEE damage patterns. Second, we performed subregion optimization based on cast-in-situ (CIS) restoration, and technical optimization by utilizing prefabrication and assembly technology (PAT). Third, the CIS/PAT UEE emergency restorability functions were constructed based on these optimizations and the local assembly capacity. Finally, the performance of the CIS/PAT restoration, optimization effect, and local assembly capacity were analyzed using a case study. The results indicated that (1) meticulous subregion optimization significantly reduced environmental work with a 13.5% speed up; (2) technical optimization incorporating PAT had the highest efficiency for improving UEE emergency restorability; (3) PAT restoration enhanced the structural resilience and functional resilience of the UEE by at least 28.34% and 62.27% over CIS restoration, respectively; (4) upper and lower thresholds exist for assembly speed in PAT restoration; (5) there exist three types of assembly capacity in PAT restoration: ring-quantity-sensitive, ring-weight-sensitive, and insensitive; and (6) the adaptive schemes maximized the performance of different local assembly capacities in PAT restoration. The UEE emergency restorability function provides a quantitative assessment tool for the resilience of UEE and a resilience enhancement scheme for disaster reduction. **DOI: 10.1061/NHREFO.NHENG-1745.** © *2023 American Society of Civil Engineers.*

Author keywords: Underground engineering environment (UEE); Emergency restorability; Prefabricated component; Prefabricated underground structures; Local assembly capacity; Adaptive scheme.

Introduction

Modern urbanization promotes the synergistic development of aboveground and underground spaces (Ma et al. 2023), which leads to a closer relationship between underground engineering and cities in terms of resilience (Liu et al. 2021a). Specifically, underground engineering is increasingly integrated within a complex urban system into an underground engineering environment (UEE) (Zhou et al. 2020) (Fig. 1). When underground engineering suffers a major disaster, its disaster effects will trigger linked damage to surrounding buildings and infrastructure. This is a coupled disaster effect that requires a specific consideration for UEE (Li and Chen 2020). The rapid construction of underground engineering has triggered many engineering accidents (Chang et al. 2001; Shi and Li 2015). Statistics for China from 2002 to 2018 provided by Yu et al. (2019) showed that underground engineering accounted for approximately half of the underground accidents.

Li et al. (2014) analyzed 118 underground engineering accidents and found that the most important hazard source was collapse accidents. This triggers chain damage to the surrounding buildings, roads, and pipelines. Thus, UEE restoration not only includes environmental and structural restoration works but also implies resilience recovery of urban systems after disasters. The fact that it took a year to fully restore a Japanese subway station after an earthquake proved the difficulty of UEE restoration (An et al. 1997). The complexity and systemic nature of UEE restoration have posed difficulties for UEE resilience studies and disaster reduction. There is still little literature on the restorability of UEE and its disaster risk reduction schemes. Therefore, the theories of urban resilience lack a crucial link. To fill this gap, this study developed the first function for UEE emergency restorability. Modern prefabrication and assembly technology (PAT) was employed to enhance UEE emergency restorability and reduce disaster impact.

Based on the preceding discussion, it is necessary to assess the restorability of urban engineering, propose specific restoration

[1]College of Civil and Transportation Engineering, Shenzhen Univ., Shenzhen 518060, China; Shenzhen Key Laboratory of Green, Efficient, and Intelligent Construction of Underground Metro Station, Shenzhen 518060, China; Key Laboratory for Resilient Infrastructures of Coastal Cities (MOE), College of Civil and Transportation Engineering, Shenzhen Univ., Shenzhen 518060, China (corresponding author). ORCID: https://orcid.org/0000-0002-8443-509X. Email: tongqiuszu@qq.com

[2]Professor, College of Civil and Transportation Engineering, Shenzhen Univ., Shenzhen 518060, China; Shenzhen Key Laboratory of Green, Efficient, and Intelligent Construction of Underground Metro Station, Shenzhen 518060, China; Key Laboratory for Resilient Infrastructures of Coastal Cities (MOE), College of Civil and Transportation Engineering, Shenzhen Univ., Shenzhen 518060, China. ORCID: https://orcid.org/0000-0002-0880-579X. Email: xschen@szu.edu.cn

[3]Professor, College of Civil and Transportation Engineering, Shenzhen Univ., Shenzhen 518060, China; Shenzhen Key Laboratory of Green, Efficient, and Intelligent Construction of Underground Metro Station, Shenzhen 518060, China; Key Laboratory for Resilient Infrastructures of Coastal Cities (MOE), College of Civil and Transportation Engineering, Shenzhen Univ., Shenzhen 518060, China. Email: sudong@szu.edu.cn

Note. This manuscript was submitted on August 22, 2022; approved on January 23, 2023; published online on March 23, 2023. Discussion period open until August 23, 2023; separate discussions must be submitted for individual papers. This paper is part of the ***Natural Hazards Review***, © ASCE, ISSN 1527-6988.

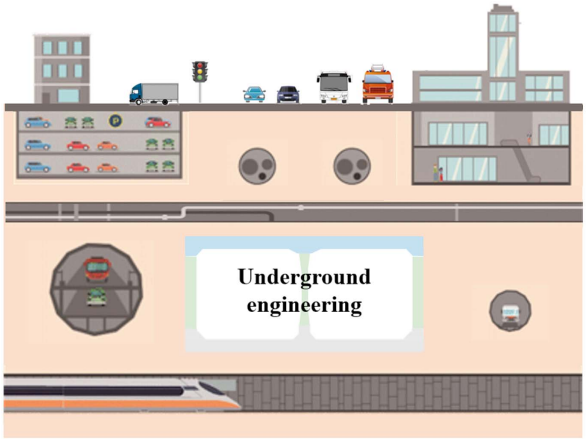

Fig. 1. Underground engineering environment.

schemes, and develop assessment methods for UEE. Urban engineering restorability has attracted widespread research interest. Zorn and Shamseldin (2015) statistically averaged postdisaster recovery curves for a variety of engineering to determine the likely recovery rates for future disasters. Sun and Zhang (2020) established a framework for assessing urban infrastructure after accidents, which facilitated the development of restoration resource allocation and optimization strategies. Tomar and Burton (2021) proposed a risk-based framework for the postearthquake functional loss and recovery assessment of urban engineering.

In addition, scholars have focused on the correlation of urban engineering restorability, which is reflected in the interdependence of the restoration of underground engineering and the surrounding environment. Ouyang and Wang (2015) developed an urban engineering multisystem restoration model and analyzed the respective restorative contributions. Zhang et al. (2018) proposed an approach for allocating restoration resources to enhance the resilience of interdependent urban engineering systems. Kong et al. (2021) developed a resilience framework that considered the interdependencies among urban engineering systems and the limitations of specialized resources.

In summary, most of the current research on urban engineering resilience focused on developing mathematical models for optimization strategies. However, these models are inapplicable to the study of specific restoration processes and schemes for UEE. Furthermore, current research on restorability mostly focused on aboveground structures, such as aboveground infrastructure (Makisha 2016), bridges (Mitoulis et al. 2021), and multiple types of buildings (Preciado et al. 2020; Joyner et al. 2021). Few systematic studies have been conducted on the emergency restorability of the UEE after disasters (Huang et al. 2022). Therefore, this study considered the correlation between the processes of environmental restoration and structural restoration and established specific UEE restoration schemes and restorability functions.

To conduct research on UEE restoration schemes, it is necessary to study the current structural restoration techniques and assess their adaptability to underground engineering restoration. Current research on structural strengthening and restoration techniques have established systematic results within the following research domains: (1) section enlargement reinforcement (Sthapit and Sthapit 2021); (2) steel component strengthening (Borri et al. 2019) (Xu et al. 2018); (3) carbon fiber reinforcement (Mohammed et al. 2020; Shabana et al. 2021); (4) shape memory alloys (SMA) component reinforcement (Xiang et al. 2020; Liu et al. 2021b); (5) steel wire composite reinforcement (Ma et al. 2021; Zhou et al. 2021); and (6) additional support and metal damping reinforcement (Zhou et al. 2021; Ren et al. 2021). Summarizing the status of research on typical structural restoration measures, these solutions may not be appropriate for UEE restoration. First, the current restoration domains have not considered the restoration of the surrounding environment. Second, the construction space of the UEE restoration is different from that of an aboveground project. It requires excavation and pit protection to expose the operation platform. Finally, the UEE damage pattern of interest in this study involved reconstruction of the collapse level. Accordingly, this study considered the environmental and structural restoration to reflect the properties of UEE restoration completely and accurately.

This study proposed a technology optimization method to achieve rapid UEE restoration. PAT has played an important role in emergency response projects during recent major disasters. In response to the COVID-19 outbreak, PAT was used to rapidly build emergency hospitals in China (Chen et al. 2022). Furthermore, PAT was used for emergency restoration of infrastructure, such as dams (Zhang et al. 2020) and bridge projects (Yuan et al. 2021). Additionally, modern PAT has exhibited fast and accurate properties. China used PAT to construct a 31.86-t nuclear infrastructure roof (Chinacrane.net 2012) and upgraded it to 220-t weight and millimeter accuracy in the latest record (SOHU.com 2018).

In summary, PAT has shown advantages of being fast, efficient and accurate in emergency restoration projects. This study is the first to propose the application of PAT to UEE restoration instead of traditional cast-in-situ (CIS) restoration (Sthapit and Sthapit 2021). Moreover, this study established the emergency restoration process and scheme specifically for UEE. Finally, a methodology for assessing PAT restoration on UEE and its optimization effect compared with CIS restoration was established. The techniques, schemes, and assessment method proposed provide application value for UEE resilience.

The assembly structure is the core of the rapid restoration of the UEE. Currently, PAT has been used in many actual prefabricated underground structures in Beijing (Cao et al. 2018), Shanghai (Zhang et al. 2021), Changchun (Yang and Lin 2021), Qingdao, and Shenzhen (Tencent 2021) in China. Based on the practical application, scholars have focused on the performance of prefabricated underground structures, and the major research results include the following studies. Ding et al. (2019) indicated that prefabricated underground structures showed good deformation resistance and mechanical properties during earthquakes. Tao et al. (2019) showed that a prefabricated underground structure maintained a relatively stable state during earthquakes using shaking table tests. Yang and Lin (2021) showed that a prefabricated underground structure exhibited promising static and dynamic bearing capacities. Based on the current research, prefabricated underground components have the capacity for mass production and application, and prefabricated underground structures have a reliable long-term operation capacity. Therefore, the development of prefabricated underground structures is supported this study to propose the application of PAT for rapid UEE restoration. The UEE emergency restorability function not only fills the gap in the resilience theory of underground engineering system but also provides strategies and practical values for resilient urban operations.

Methodology

This study aimed to evaluate UEE emergency restorability and PAT restoration. First, the restoration levels were classified based on the UEE damage pattern. Second, subregion optimization was performed based on the restoration level and CIS restoration case,

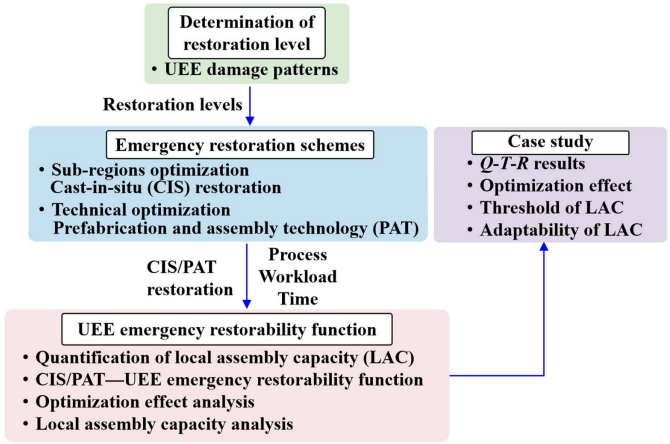

Fig. 2. Methodological path.

and technical optimization was performed based on PAT technology. The CIS/PAT emergency restoration schemes were constructed to obtain the restoration process, workload, and time. Third, the CIS/PAT UEE emergency restorability functions were constructed based on the aforementioned factors and local assembly capacity. Finally, the functions were used in combination with the case study and to support the optimization effect analysis and local assembly capacity analysis (Fig. 2).

Determination of Restoration Level

Damage levels in different regions of the UEE are generally inconsistent. Different restoration measures for different damage levels are conducive to the rational allocation of emergency restoration resources and acceleration of the restoration progress. The core of determining the damage level is to define the impact of the underground engineering on the surrounding environment, particularly the chain damage effect. For limited environmental impacts and structural damage, this study advocated partial restoration or structural reinforcement to minimize environmental disturbance. In addition, the determination is based on UEE having the regular structural sections, such as underground stations, pipe culverts, and tunnels. It is appropriate to divide the restoration region into several areas with regular sections when defining the restoration levels.

The damage patterns of the UEE were used as the basis for determining the restoration levels, which were classified into four levels as shown in Fig. 3. These levels are as follows:

- Collapse: this level of damage triggers a chain damage effect on the surrounding environment. It is necessary to consider the recovery of the surrounding environment and the reconstruction of the structure after overall earth excavation.
- Severe: at this level of damage, the structure can still stand, and the surrounding environment may only be partially disturbed or remain intact.
- Moderate damage: the structure requires a significant restoration and the surrounding environment remains intact.
- Minor damage: the structure requires a minor restoration and the surrounding environment remains intact.

Moderate and minor damage were combined as reinforcement levels. In summary, corresponding to the UEE damage patterns, emergency restoration schemes were classified into three levels; the highest level was reconstruction, followed by partial restoration and finally reinforcement.

Emergency Restoration Schemes

After determining the restoration levels, this study obtained emergency restoration schemes through subregion optimization and technical optimization. Subregion optimization included subregion planning and process reduction, whereas technical optimization included the adoption of a prefabricated underground structure and an assembly construction plan. After optimization, the PAT restoration plan was developed, and the CIS restoration plan was used for comparison.

Subregion Optimization

The primary aspect of subregion optimization is subregion planning. Fig. 3 shows that each restoration level corresponds to a different restoration scale, with the most intensive reconstruction level involving extensive environmental and geotechnical work. Each restoration level established its own subregions, which were subregions for reconstruction, partial restoration, and reinforcement. Each subregion had a specific range and process. Owing to the standardization of the underground engineering cross section, the longitudinal dimensions of the restoration region can be used to assess the workload and recovery time of the subregions. Specifically, the reconstruction subregion was considered to perform the heaviest environmental and structural restoration processes.

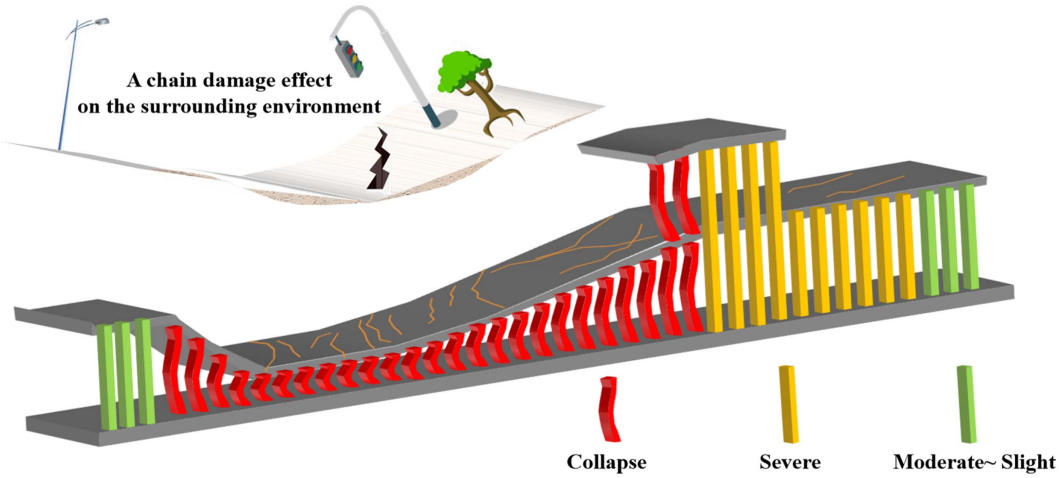

Fig. 3. UEE damage patterns.

Table 1. Construction process of three subregions

Type	Process	Subject	Subregions		
			CIS reconstruction	Partial restoration	Reinforcement
ENV	Presurvey	Surrounding buildings, upper facilities, roads, underground infrastructure, geotechnical environment, and so on	Reconstruction	Reconstruction	Reconstruction
	Upper obstacle clearance		Reconstruction	Not required	Not required
	Pipeline restoration and temporary road traffic restoration		Reconstruction	Not required	Not required
	Emergency protection		Reconstruction	Partial construction	Partial construction
	Diaphragm wall construction		Reconstruction	Not required	Not required
	Grouting engineering		Reconstruction	Not required	Not required
	Excavation works		Reconstruction	Partial construction	Not required
	Precipitation engineering		Reconstruction	Partial construction	Not required
STR	Construction platform engineering	Underground engineering	Reconstruction	Not required	Not required
	Structural demolish		Reconstruction	Partial construction	Not required
	Structural restoration		Reconstruction	Partial construction	Partial construction
	Waterproof engineering		Reconstruction	Not required	Not required
ENV	Earthwork backfilling works	Road and upper facilities	Reconstruction	Partial construction	Not required
STR	Construction of equipment and auxiliary structures	Underground engineering	Reconstruction	Not required	Not required
ENV	Road restoration and municipal restoration	Road and upper facilities	Reconstruction	Not required	Not required

Note: ENV = surrounding environment restoration process; and STR = internal structure restoration process.

The most dominant process in the reconstruction environmental restoration process was the diaphragm wall construction and excavation work (Civil Engineering Department 1997). There is a correspondence between the reconstruction environmental restoration process and the dimensions of the reconstruction area. Therefore, the reconstruction workload can be optimized through clear and detailed subregion planning of the reconstruction region.

Another key aspect of subregion optimization is process reduction. The UEE benchmark process was constructed based on the emergency CIS restoration scheme (Civil Engineering Department 1997). The benchmark processes were divided into environmental and structural restoration processes, and the restoration subjects corresponding to the processes were summarized (columns labeled Type and Subject in Table 1). Furthermore, the processes for partial restoration and reinforcement can be optimized, particularly for numerous environmental restoration processes. Depending on the construction needs, the results of the process reduction are shown as partially performed or not required. By applying hierarchical and refined process reduction, extensive environmental and structural restoration processes and workload of the UEE were reduced.

The construction processes of the three subregions of the emergency restoration schemes after subregion optimization are summarized in Table 1. The reconstruction subregion has many processes that were fully performed. Particularly, the workload for reconstructing the surrounding environment is significant and requires substantial restoration time. In comparison, partial restoration and reinforcement can be accomplished earlier after process reduction. Historically, the restoration time was proven to depend on the reconstruction progress, and both partial restoration and reinforcement were completed early (*Sankei Shimbun* 1995). Therefore, reconstruction works dominated UEE restoration and determined the recovery time. Accordingly, the key to enhancing UEE emergency restorability is to improve reconstruction capacity. The CIS Reconstruction column of Table 1 can be used as the original emergency restoration scheme.

Technical Optimization

The primary aspect of technical optimization is the adoption of a prefabricated underground structure to promote easy and rapid construction. Technical optimization adopts a combination of the old and new structures, that is (1) the original damaged structure is demolished as needed, and the maximum demolition is to retain at least the original baseplate; (2) the assembled joints are formed in the baseplate through small casting, and the baseplate is restored; and (3) the prefabricated walls, columns, and roofs are constructed by PAT, and the original baseplate is assembled with prefabricated components to generate a prefabricated underground structure (Fig. 4). This technical optimization not only reduces the heavy workload of the new-built baseplate but also uses PAT to assemble the new structure above the baseplate quickly.

Another key aspect of technical optimization is the adoption of an assembly construction scheme. Based on the aforementioned prefabricated underground structure, this study used assembly construction to accelerate restoration. The traditional CIS restoration process consumed considerable effort and time, including onsite welding of new and old reinforcements, new construction platforms, formwork, and steel skeleton construction, pouring concrete, and waiting for maintenance (Civil Engineering Department 1997). In comparison, with the application of industrialized prefabricated components, restoration requires only assembly construction onsite, reducing a significant amount of CIS processes and time. In addition, PAT restoration eliminated the need to build construction platforms because it avoided large-scale onsite casting. Finally, PAT provided waterproofing by preinstalling strips at the assembled joints (Yang and Lin 2021), thus reducing waterproofing work. Fig. 5 presents a detailed description of the PAT reconstruction scheme.

In the figure, Step 1 is restoration of surrounding environment, which is carried out first. Emergency support is required in the collapse region, and then excavation is carried out to underground engineering for demolition. In Step 2, when demolishing damaged vertical members, 1 m of component ends are retained to expose existing steel rebars. Additional reinforcement and existing steel rebars are welded together. Small-scale casting forms tenon-mortise joints when the baseplate is restored. In Step 3, prefabricated components are hoisted for construction. First, the prefabricated walls and columns are lifted to the joints for assembly. Then, the prefabricated roof is lifted and assembled with truck cranes. Finally, the

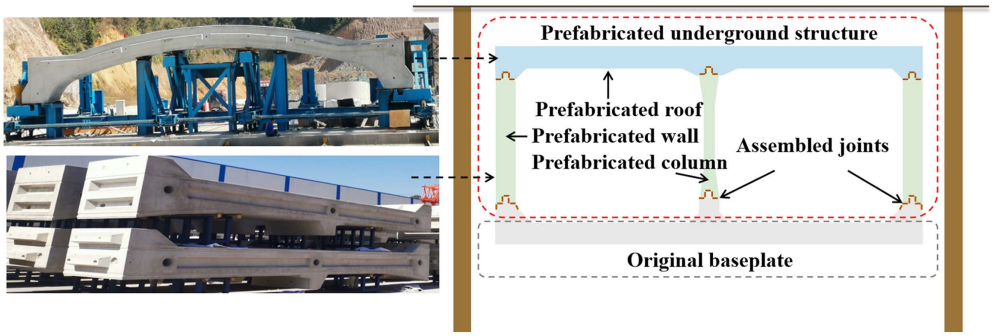

Fig. 4. Prefabricated underground structure with prefabricated components. (Images by authors.)

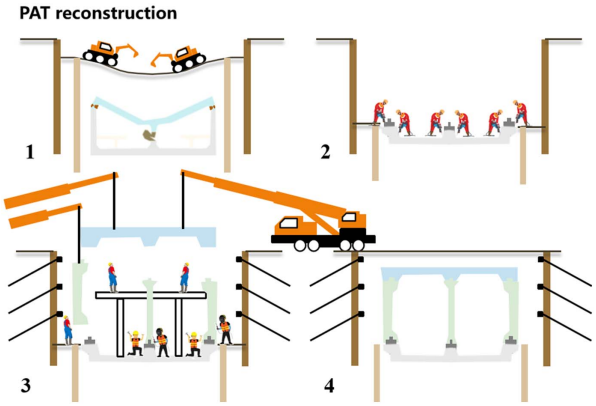

Fig. 5. Process of PAT reconstruction.

prefabricated roof is positioned on the prefabricated walls and columns for assembly. In Step 4, after completing the main structure reconstruction, the soil is backfilled, and the road surface is restored.

In summary, the core of technical optimization is the transformation of CIS restoration into PAT restoration. The optimized subregion construction process, structural system, and construction plan of the PAT emergency restoration are presented in Table 1 and Fig. 5, respectively. Compared with CIS restoration, subregion optimization meticulously divided the reconstruction subregion and significantly reduced massive environmental restoration processes. Additionally, the application of the prefabricated underground structure and assembly construction significantly reduced the time-consuming onsite pouring process. Therefore, the proposed PAT restoration scheme using the two optimizations can enhance the UEE emergency restorability.

Emergency Restorability Function

This section first quantified the local assembly capacity and constructed CIS/PAT UEE emergency restorability functions. Next, the optimization analysis process of PAT restoration was established by comparing the two functions. Finally, the threshold and adaptability analysis process of the local assembly capacity were established.

Quantification of Local Assembly Capacity

PAT restoration depends on local assembly capacity. The assembly construction time of a single ring of the prefabricated underground structure was calculated using Eq. (1) to assess assembly speed. Here, r is the lifting batch that characterizes the assembly scheme of the prefabricated underground structure. The vertical components are lifted and positioned before the horizontal components. Therefore, the vertical and horizontal components were divided into two batches. N_{Lr} is the number of components in a batch related to the prefabricated underground structure. For example, the number of vertical components and the roof of the prefabricated single-ring structure in the 1F area are $N_{Lr} = 3$ and 1, respectively. T_{Lr} is the lifting time of a single component. This parameter is closely related to the local assembly capacity, equipment resources, and restoration cost, which determines PAT assembly speed. T_{Sr} is the stopping time of this batch and is related to the restoration workload of the process

$$T_{1R} = \sum_{k=1}^{r} (N_{Lr} T_{Lr} + T_{Sr}) \tag{1}$$

Lifting weight is also an important parameter for PAT restoration. A component with a large mass reduces the efficiency of transporting and lifting precast components; a small component mass with too many joints also affects the speed of the onsite assembly. The achievable assembly speed within a specific lifting-weight range represents the local assembly capacity.

CIS/PAT UEE Emergency Restorability Function

UEE emergency restorability functions were constructed to evaluate the recovery performance and duration of UEE emergency restoration. The CIS UEE emergency restorability function, based on the actual CIS restoration process of Daikai Station, was first established to consider the integrity and complexity of UEE restoration (Civil Engineering Department 1997). The total workload and process restoration time were evaluated using the longitudinal dimensions of the reconstructed region. The restoration processes and recovery times are listed in Table 2.

The PAT UEE emergency restorability function was established based on the CIS UEE emergency restorability function and the PAT restoration scheme. The process is as follows. First, the PAT restoration processes were subject to subregions and technical optimization. The PAT restoration process time (t_j) was derived based on the workload and recovery time (T_i) of CIS restoration. After subregion optimization, the longitudinal dimension of the PAT reconstruction region was reduced. Its ratio to the longitudinal dimension of CIS restoration was used as the optimized ratio (η_i) of the workload and recovery time. For technical optimization, PAT restoration adopted a prefabricated underground structure and an assembly construction scheme, t_{14} and t_{18} characterized the PAT assembly process times in the 1F and 2F areas, respectively, obtained by dividing the quantity of prefabricated structural rings by the individual ring assembly speed [Eq. (1)]. Because some of the processes were eliminated, the PAT restoration process skipped

Table 2. CIS/PAT restoration Q-T assessment process

Process i	CIS restoration	PAT restoration	Q_S	Q_F	T_i	t_j	Correlation
1	Preparation work	Reconstruction	Collapse or	0	T_1	$\eta_1 T_1$	—
2	Diaphragm wall construction with grouting engineering	Reconstruction	severe status		T_2	$\eta_2 T_2$	4, 7
3	Excavation work	Reconstruction			T_3	$\eta_3 T_3$	—
4	Anchor bar works	Reconstruction			T_4	$\eta_4 T_4$	—
5	Construction platform works	Not required			T_5	0	—
6	Support work	Reconstruction			T_6	$\eta_6 T_6$	—
7	Precipitation engineering	Reconstruction			T_7	$\eta_7 T_7$	8
8	Grouting work	Reconstruction			T_8	$\eta_8 T_8$	9
9	2F area demolition work	Reconstruction			T_9	$\eta_9 T_9$	10
10	1F area demolition work	Reconstruction			T_{10}	$\eta_{10} T_{10}$	11
11	Removal of sidewall and center column	Reconstruction			T_{11}	$\eta_{11} T_{11}$	12
12	Construction platform engineering	Reconstruction			T_{12}	$\eta_{12} T_{12}$	13
13	Implant and weld steel bar	Reconstruction	Recovering		T_{13}	$\eta_{13} T_{13}$	14
14	CIS engineering	Early-strength concrete joint construction			T_{14}	$t_{13} = 7$	15
15	Central column restoration works	Assembly construction			T_{15}	t_{14}	16
16	Steel central column grouting concrete				T_{16}		17
17	Sidewall waterproofing works	Not required			T_{17}	—	18
18	Roof waterproofing works	Not required			T_{18}	—	Rail opening
	Rail opening	Reconstruction	1F area recovered	a_1	—	—	19
19	Rest phase	Reconstruction	2F area recovering		T_{19}	$t_{15} = T_{19}$	20
20	Baseplate reinforcement	Reconstruction			T_{20}	$\eta_{20} T_{20}$	21
21	Baseplate and foundation construction	Reconstruction			T_{21}	$\eta_{21} T_{21}$	22
22	CIS and waterproofing construction in 2F area	Assembly construction			T_{22}	t_{18}	23
23	Construction of equipment and auxiliary structures	Reconstruction			T_{23}	$t_{19} = T_{23}$	Station opening
	Road and municipal restoration						
	Backfill works						
	Station opening	Reconstruction	1F area and 2F area recovered	$a_1 + a_2(1 + Q_{FSUM})/N_S$	—	—	—

Note: Process 1, preparation work, includes a presurvey, upper obstacle clearance, pipeline restoration, road traffic, and emergency protection. Q_{FSUM} = sum of the other stations' Q_F.

Processes 5, 17, and 18 of the CIS restoration and performed the next process.

The UEE emergency restorability function advances the structural and functional performance Q and process time T strictly corresponding to the restoration process (Fig. 6). There is a correlation between partial processes, which implies that the completion of these processes determines the start of certain processes. For example, the completion of diaphragm wall construction (Process 2) determines the start of the anchoring and precipitation work (Processes 4 and 7). These processes together established the time chain for full restoration and were therefore denoted as key processes. The relationship between of the key process were integrated to construct a recovery time chain of emergency restoration functions. Finally, a resilience function R, was designed to evaluate the quantitative performance of the restoration schemes. The Q-T-R function established a quantitative assessment process for the emergency restorability of the UEE, and the steps are as follows:

1. Q_S was set to characterize the recovery of structural performance. Q_F was set to characterize the recovering traffic function state of the rail and station.
2. Q_S was jointly evaluated based on vulnerability and restorability. Q_S and T strictly corresponded to the restoration processes. For example, the Q_S of the collapsed UEE is zero when disaster strikes; structural restoration is on standby when environmental work is in progress, and Q_S evolution tends to be a constant zero (Processes 1–12); after the structure restoration is initiated, the restoration processes of concrete, reinforcement, and steel works (Processes 13–18 and 19–21) restore Q_S and consume a definite recovery time; finally, Q_S recovers to 1 or higher, as indicated in the Q_S and T_i columns in Table 2.
3. Q_F was jointly evaluated by the surrounding environment and substructure's Q_S. The recovery of Q_F had a definite relationship with the multiple Q_S values. Based on experience from the Daikai Station case, certain operational functions of the line and station were restored when key Processes 18 and 23 were completed. Therefore, Q_F is related to the Q_S of Processes 18 and 23, as indicated in the Q_F column in Table 2. Experience has also shown that restoring line functions is critical to urban resilience. Traffic function was fully restored after the subsequent restoration of multiple stations. Q_F characterized the comprehensive functional state of the rail and multiple stations by Eq. (2)

$$\boldsymbol{Q}_F = a_1 \boldsymbol{Q}_{F\text{-Rail}} + a_2 \frac{\sum_{i=1}^{n} \boldsymbol{Q}_{F\text{-Station } i}}{\boldsymbol{N}_S} \tag{2}$$

If Q_F only considers the restoration of the station itself, N_S takes a value of 1.

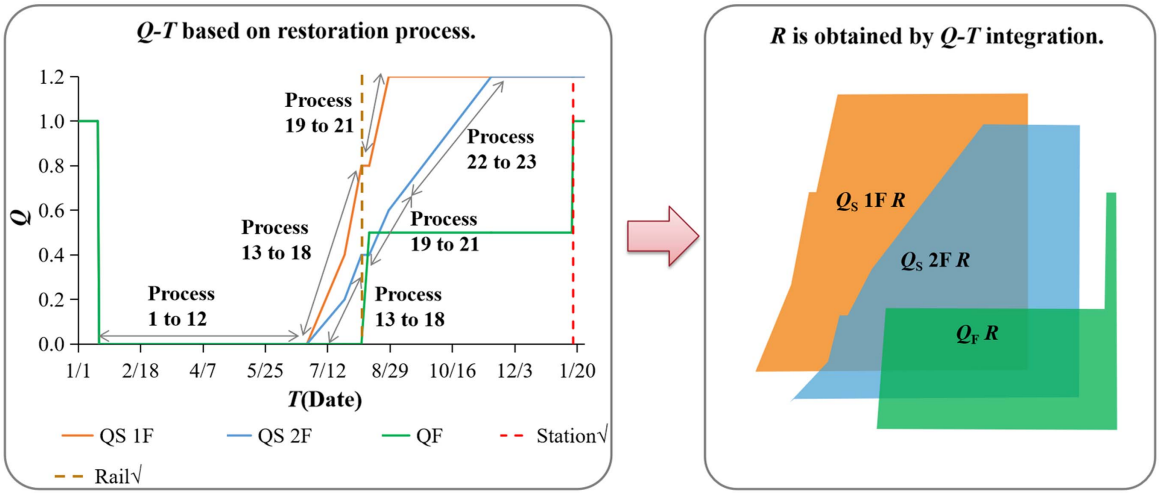

Fig. 6. UEE emergency restorability function. The restoration process refers to Table 2.

4. Q_S-T and Q_F-T functions were constructed by projecting the time sequence of disaster effects and restoration processes onto the T axis and mapping their corresponding Q.
5. Q_S-T and Q_F-T functions were integrated to obtain the respective resilience function R

$$\boldsymbol{R} = \frac{\int_{t_0}^{t_{\max}} \boldsymbol{Q}(t)dt}{(\boldsymbol{t}_{\max} - \boldsymbol{t}_0)\boldsymbol{Q}(0)} \tag{3}$$

where $Q(t) = Q_S$ or Q_F over time; and t_0 and $t_{\max}$ = times when the disaster starts and the maximum recovery time of multiple schemes, respectively.

Optimization Effect Analysis

Based on a comparison of the CIS/PAT UEE emergency restorability function, we analyzed the optimization effect of the PAT emergency restoration scheme. The calculation process is as follows:

1. In comparison with CIS restoration, the optimization effect of PAT restoration included the workload and recovery time. The recovery time was used as a representative parameter for the optimization analysis because of the linear mapping workload optimization.
2. T_O is the optimization time for each process of PAT restoration, and T_{com} is the cumulative optimization time for key processes from the beginning to process m.
3. The total cumulative optimization time was classified into two parts: T_{COS} for subregion optimization and T_{COT} for technological optimization.
4. The aforementioned optimization time was divided into two phases: the rail restoration phase and the station restoration phase.

These steps are expressed by Eqs. (4)–(9)

$$\boldsymbol{T}_{Oi} = \boldsymbol{T}_i - \boldsymbol{t}_j \tag{4}$$

If the process is correlated, then

$$\boldsymbol{T}_{COm} = \sum_{i=1}^{m} \boldsymbol{T}_{Oi} \tag{5}$$

In the rail restoration phase

$$\boldsymbol{T}_{COS} = \boldsymbol{T}_{CO12} \tag{6}$$

$$\boldsymbol{T}_{COT} = \sum_{i=13}^{18} \boldsymbol{T}_i - \sum_{j=12}^{14} \boldsymbol{t}_j \tag{7}$$

In the station restoration phase

$$\boldsymbol{T}_{COS} = \boldsymbol{T}_{CO22} - \boldsymbol{T}_{CO18} \tag{8}$$

$$\boldsymbol{T}_{COT} = \boldsymbol{T}_{22} - \boldsymbol{t}_{19} \tag{9}$$

Local Assembly Capacity Analysis

Local assembly capacity is a multifactor parameter controlled with respect to the functional recovery time and structural restoration process time of the UEE. Local assembly capacity determines the efficiency of technical optimization, and it is necessary to determine the key factors and corresponding thresholds. The threshold analysis of local assembly capacity was performed using the following process:

1. The local average assembly quantity (per hour) of prefabricated underground structure rings was used as a variable and substituted into Eq. (1) to quantify local assembly capacity.
2. The process time corresponding to local assembly capacity was input to the PAT UEE emergency restorability function, and Eqs. (6)–(9) are used for optimization analysis.
3. A parametric analysis was performed for PAT restoration in comparison with CIS restoration, and the local assembly capacity thresholds were obtained after exploring the key factors.

Another key issue for PAT emergency restorability is the competing relationship between the local assembly speed and lifting weight. An ideal local construction scheme should be able to construct wider and fewer prefabricated structural rings as quickly as possible. Conversely, the structural ring width would have to be reduced, and the ring quantity should be increased to accommodate the local assembly capacity. This study advocated designing the width of the prefabricated structural ring according to different local assembly capacities to achieve mutual coordination between the design and construction. Therefore, the adaptability analysis of local assembly capacity was performed using the following process:

1. Through investigation, the assembly times of representative maximum and minimum weight components were considered for the characterization of local assembly capacity.

2. The assembly time of components with different ring widths was calculated by the interpolation of the assembly speeds of maximum and minimum weights, as in Eq. (10).
3. A certain series of assembly speeds was taken as variables and substituted into Eq. (1).
4. The corresponding assembly process time was inputted to the PAT UEE emergency restorability function to analyze the total assembly time under different ring widths.

Finally, an adaptive scheme matching the design and construction was used to maximize the PAT UEE emergency restorability

$$T_{M_x Lr} = \frac{M_x - M_{\max}}{M_{\min} - M_{\max}} T_{M_{\min} Lr} + \frac{M_x - M_{\min}}{M_{\max} - M_{\min}} T_{M_{\max} Lr} \quad (10)$$

Case Study and Results

This section uses Daikai Station emergency restoration for a case study. First, the restoration levels of the Daikai Station were determined. Furthermore, this section adopted the UEE emergency restorability function to conduct performance-time-resilience assessment and optimization effect analysis. Finally, the local assembly capacity threshold and adaptability analysis were performed on the case.

Description of Case Underground Engineering

The earthquake that struck Hyogo, Japan, on January 17, 1995, caused a loss of more than 6,300 lives. The earthquake caused severe damage to lifeline facilities in the Kobe area, most notably to the subways. The earthquake caused massive damage to at least five subway lines in Kobe city. Daikai Station of the Kobe subway collapsed and triggered significant chain damage to the surrounding environment. The emergency restoration of Daikai Station during a disaster was considered as a case study. The original CIS restoration was used for comparative analysis with the PAT restoration.

The plane and section view of the Daikai Station are shown in Fig. 7. The station had a 2-story underground structure. The rail area (Section 1-1, 1F area) was a 1-story, 2-span frame construction with width of 17 m, height of 7.17 m, and a 4.8-m soil cover. The height of the center column was 3.82 m and the cross section was 0.4 × 1.0 m, 3.5 m apart. The heights of the top and bottom beams were 1.6 and 1.75 m, respectively. The thicknesses of the roof and baseplate were 0.80 and 0.85 m, respectively. The thickness of wall was 0.7 m above the platform and 0.85 m below the platform. The lobby area (Section 2-2, 2F) was a 2-story, 4-span frame construction with a width of 26 m and a height of 10.12 m. The covering soil thickness was 1.9 m, and the wall thickness was 0.50 m.

After the earthquake, the surrounding environment within 30 m of the station was surveyed. Most of the surrounding buildings were 3–5 stories, and there were cases of collapse and inclination to slight damage because of the earthquake. The road surface was severely damaged by road subsidence. The upper road facilities, electric poles, and signal lights were damaged. Many types of underground infrastructure, such as gas lines, electric power lines, sewage pipes, water pipes, trunk rail lines, and communications lines, were seriously damaged by road subsidence.

Restoration Levels and Schemes Determination

The restoration levels of the postdisaster damage patterns at Daikai Station were determined. Reconstruction was performed in collapsed regions, partial restoration was performed in severely damaged regions, and reinforcement was performed in the remaining regions (Fig. 8). Each restoration-level region constructed its own subregion. After the subregion optimization, the reconstruction lengths of 1F and 2F regions were 68.3 and 23.6 m, respectively. The results showed that the perimeter length of the environmental works (such as the length of the diaphragm wall and anchor arrangement) was only 0.56 times that of the original scheme, and the length of the structural works was 0.71 times that of the original scheme. The optimization effect is remarkable, as shown by the optimized ratio (η_i) in Table 3. Compared with the original CIS reconstruction, meticulous subregion optimization reduced a large amount of reconstruction work. This is a meticulous reorganization of the relationship between the station and the surrounding environment. Therefore, the analysis result indicated a restoration strategy that protects and microdisturbs the environment while avoiding large-scale restoration.

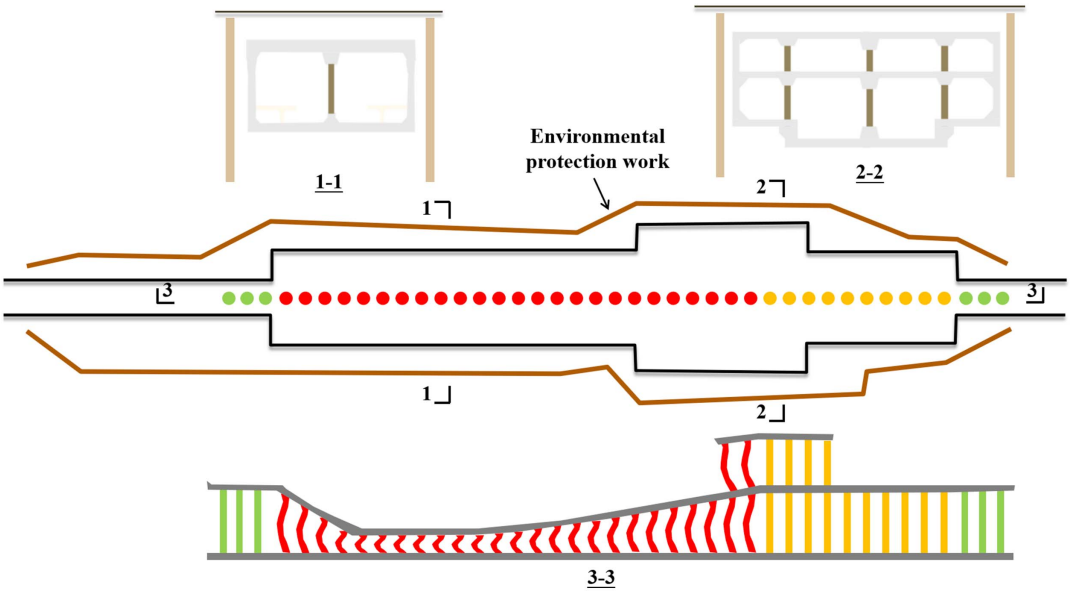

Fig. 7. Plane and section of Daikai Station.

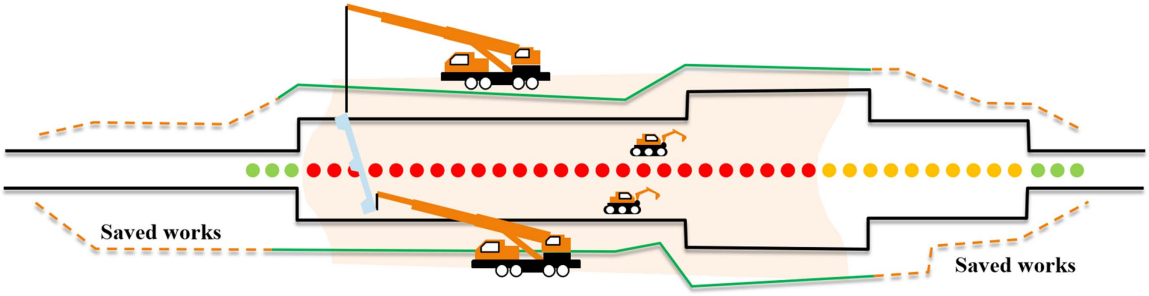

Fig. 8. Surrounding environment and internal structure works after subregion division.

Table 3. Subregions optimization

Type	Optimized process	η_i
ENV	Diaphragm wall construction	0.56
	Excavation work	0.56
	Anchor bar works	0.56
	Construction platform works	0
STR	2F area demolition work	0.4
	Removal of sidewalls and center columns	0.71
	Restoration platform construction	0.71
	Implant and weld steel bar	0.71
	Baseplate and foundation construction (with joint mortise)	0.71
	Sidewall waterproofing works	0
	Roof waterproofing works	0

For technical optimization, the reconstruction subregion adopted the PAT emergency restoration scheme and used CIS restoration for comparative analysis. Traditional CIS restoration required construction in a complex and narrow pit, especially in the 1F area (Fig. 8). Importantly, structural demolition and cleanup processes were also performed in the pit. In this case, the CIS restoration conflicted with the construction space of the previous structural processes, which was not conducive to reducing the recovery time. In comparison, PAT restoration only required lifting outside the pit and allowed crossover process with the previous process. The technical optimization considered the influence of the prefabricated underground structure and construction scheme but did not consider the optimization effect of crossover development with the previous process. PAT restoration has greater potential for improving UEE emergency restorability.

Emergency Restorability Evaluation

Performance-Time-Resilience Assessment Results

The CIS/PAT UEE emergency restorability function was established based on the aforementioned restoration levels and schemes. For subregion optimization, the PAT restoration process times were calculated based on η_i from Table 3. For technical optimization, the local assembly speed of PAT was taken as 1.1 rings/day with a width of 2 m/ring (Yang and Lin 2021). Process-T curves were constructed for comparison by applying the process of CIS/PAT restorations corresponding to the start to end dates of the processes [Figs. 9(a and b)].

The Q-T function was characterized by a distinct performance stagnation period and a rise period [Figs. 9(c and d)]. This is a result of the strict correspondence between the emergency restorability function and the process-T function [Figs. 9(a and b)]. The stagnation period reflected many environmental processes must be performed before structural restoration (Processes 1–12 in Table 2). The stagnation period of CIS restoration accounted for 76.92% of the rail restoration phase, revealing the complex and heavy environmental processes of CIS restoration. In contrast, the stagnation period of PAT restoration was 28 days (14.00%) shorter than that of CIS restoration, reflecting the effect of meticulous subregion optimization on UEE restoration.

The rise period reflected the effect of the technical optimization. For example, the slope in the 1F area of Q_S-T function at 1.1 ring/day was comparable to that of the CIS restoration, which was optimized for only 1 day. The slope in the 2F area increased significantly, indicating that 43 days was optimized. This UEE case was characterized by a large amount of restoration in the 1F area, which played a controlling role in PAT technology. The 1F area's analysis results showed that the current construction technological optimization level can be further improved.

UEE emergency restorability was quantified using the resilience function R. The structural performance resilience function R of the PAT restoration was improved by 17.17% to 28.34% over CIS restoration. In particular, the functional resilience of the PAT restoration improved by 62.27% [Figs. 9(c and d)]. The results of the resilience assessment revealed the low efficiency of the CIS reconstruction effort. In contrast, after two optimization efforts, PAT restoration has a higher potential for resilience improvement in urban traffic.

Optimization Effect

This study statistically analyzed the recovery time optimization effects of each PAT restoration process. A T-process curve was constructed corresponding to the optimization time T_O, and the cumulative optimization time T_{CO} curve was formed by accumulating T_O. From Fig. 10(a), key Processes 2, 8, 14, and 18 increased the T_{CO}, whereas Processes 3 and 4 had little effect on T_{CO} despite optimizing a large amount of T_O. This indicates that the key process forms a tight chain of recovery times, and optimizing the key process is the most efficient technique for reducing the recovery time. Fig. 10(b) shows the optimization effects and indicates the following:

- Rail restoration phase: this phase involves many environmental and structural restoration preparation steps. Subregion optimization focuses on meticulous planning of the reconstruction subregion and the reduction of massive environmental processes. Compared with CIS restoration taking 200 days, the PAT restoration subregion optimization T_{COS} reached 27 days (13.5% speedup). Therefore, subregion optimization has high optimization efficiency in the rail restoration phase.
- Station restoration phase: most environmental work was completed during the rail restoration phase; therefore, T_{COS} was only accelerated by 2 days (1.27%). Technical optimization reduces the CIS works when structural restoration is predominant.

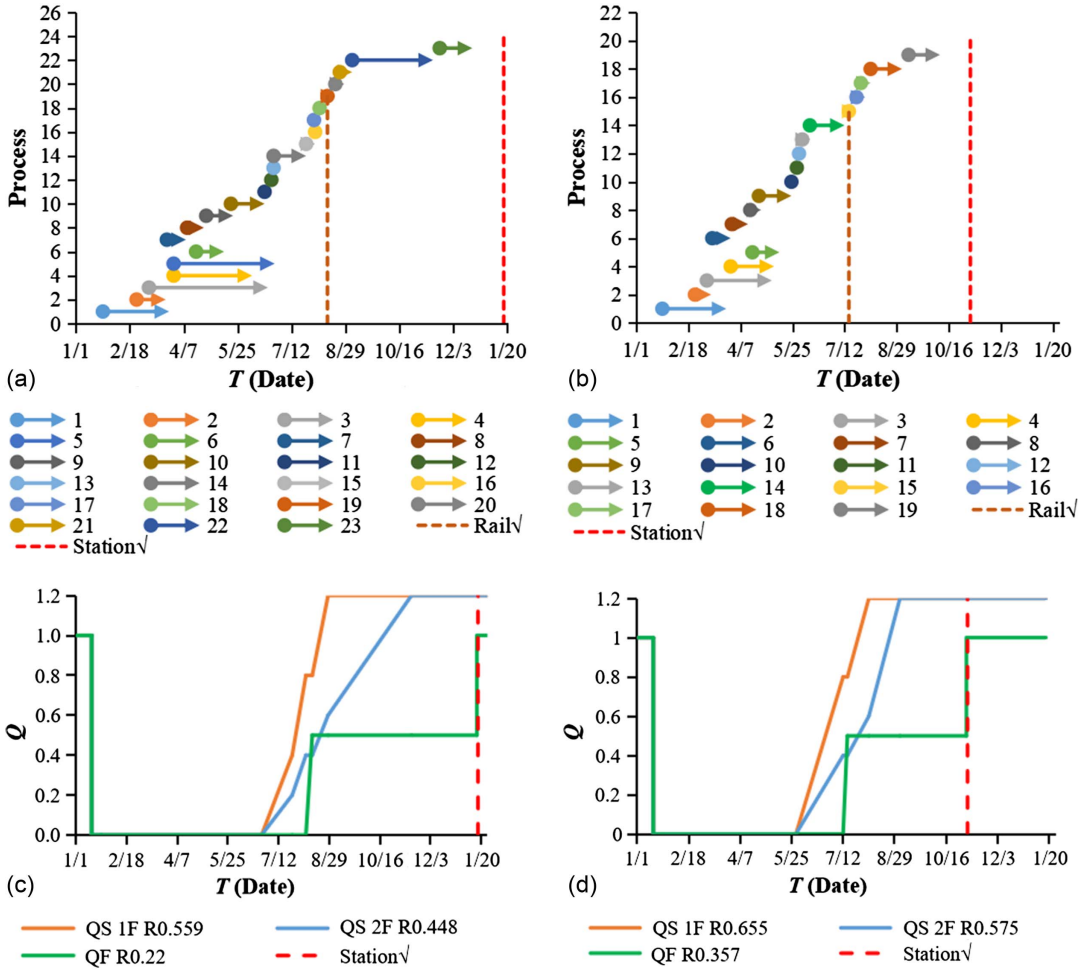

Fig. 9. Process-T and Q-T of restoration: (a) process-T for CIS restoration; (b) process-T for PAT restoration; (c) Q-T of CIS restoration; and (d) Q-T of PAT restoration. QS 1F R0.559 indicates that the structural resilience of 1F is 0.559, and QF R0.22 indicates that traffic functional resilience is 0.22.

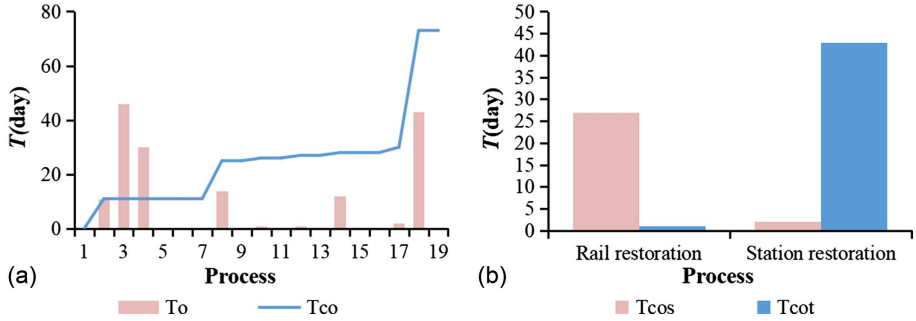

Fig. 10. Process-optimization time: (a) T-process of PAT restoration; and (b) T_{COS} and T_{COT} of PAT restoration.

The technical optimization T_{COT} reached 43 days (27.39% acceleration) compared with the CIS restoration. Therefore, technical optimization has a high optimization potential during this phase.

- Overall, compared with CIS reconstruction, the opening times for rail and stations of PAT reconstruction were 28 days (14.00%) and 73 days (28.66%), respectively. T_{COS} and T_{COT} reached 29 and 44 days, respectively, and T_{COT} accounted for at least 60.27% of T_{CO}. Technical optimization is the most effective way to improve UEE emergency restorability.

Threshold of Local Assembly Capacity

The performance of local assembly capacity in PAT restoration is affected by many factors, which are detailed subsequently. The characteristics of the T-process curve were observed by varying the local assembly speed gradually. The results showed that when the assembly speed was less than 0.4 rings/day, the rail and station recovery times of PAT restoration were later than those of CIS restoration. When the assembly speed was 0.5 ring/day, the opening time of the station was advanced, but the line recovery time was still longer than that of the CIS restoration. When the assembly speed

was 1 ring/day, both the line and station were opened earlier, but PAT technological optimization in the line restoration phase was not reflected. Specifically, when the assembly speed reached 1.1 ring/day, the recovery time of the line and station was not less than that of the CIS restoration, and technical optimization was embodied [Figs. 11(a and b)]. In this case, the corresponding R of Q_F was 59.38% larger than that of CIS restoration. Analytically, the lower limit of assembly speed is constrained by functional recovery, restoration techniques, and UEE project features. Therefore, in this case, the assembly speed of 1.1 ring/day was the lower threshold for local assembly capacity. The local assembly capacity must meet the lower limit of assembly speed for PAT emergency restorability.

Based on the assessment results, this study analyzed the effect of local assembly capacity on PAT restoration. Taking Chinese PAT data as examples, the literature indicated that 50 min/ring can be achieved in actual projects when the weight was approximately 75 t and lifting used two cranes (Luo et al. 2014), and 10 min/ring when the component weight was below 25 t (Feng 2014). The assembly speed and lifting weight represent the quantification of local assembly capacity for PAT restorability analysis. A certain construction interval ($T_{Sr} = 0.2N_{Lr}T_{Lr}$) was considered and substituted into Eq. (1).

For emergency construction projects, the upper threshold construction speed determines the recovery capability. To evaluate the upper assembly speed of the PAT restoration, the efficiency of different construction techniques was studied using the daily construction time as a variable [Figs. 12(a and b)]. From the analysis results, when a daily construction time of 4 h was achieved, at the current assembly speed, T_{CO} of more than 91 days could be achieved. In particular, when the construction time reaches 12 h (4.2 rings/day) or more, T_{CO} reached 121 days. Furthermore, the 24-h construction scheme's R was only 3.70% higher than for 12 h, indicating that the T_{COT} entered a boundary stage. At this point, increasing the daily construction time was not beneficial. Therefore, there is an upper threshold for construction speed. The goal is to refine and conserve emergency restoration resources without limiting the restoration capacity. In summary, the analysis results suggested that the upper and lower thresholds of assembly speed were 4.2 and 1.1 rings/day, and that the local assembly capacity can be met using large (under 75 t) prefabricated components (Sun 2020).

Adaptability of Local Assembly Capacity

The PAT sections of the prefabricated underground structures were determined from the actual restored station structures and compared with the aforementioned lifting weight thresholds. The prefabricated roof, walls, and columns were reinforced according to an actual scheme (Nakamura et al. 1997). The center column was enlarged at the joint areas to enhance the load-bearing capacity of the joint. The prefabricated roof was provided with a 15% section

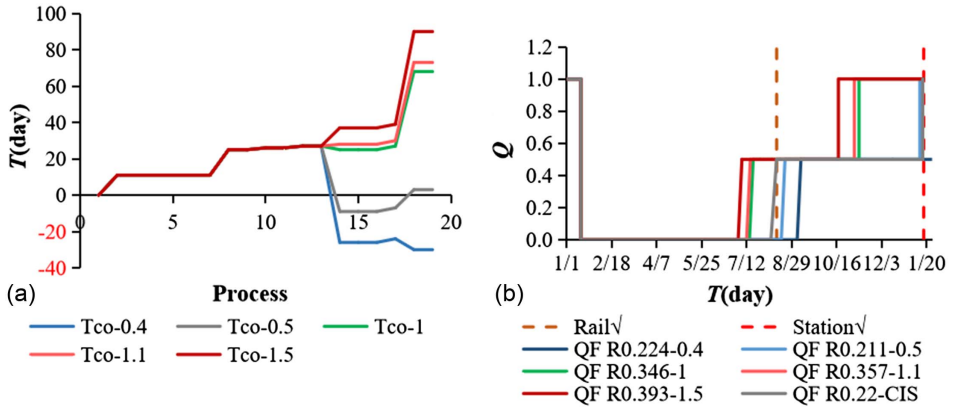

Fig. 11. Process-optimization time: (a) T-process of PAT restoration; and (b) Q_F-T of PAT restoration. Tco-0.4 represents the cumulative optimization time for 0.4 ring/day scheme. QF R0.224-0.4 represents the Q_F of the aforementioned scheme, and the functional resilience evaluation was 0.224.

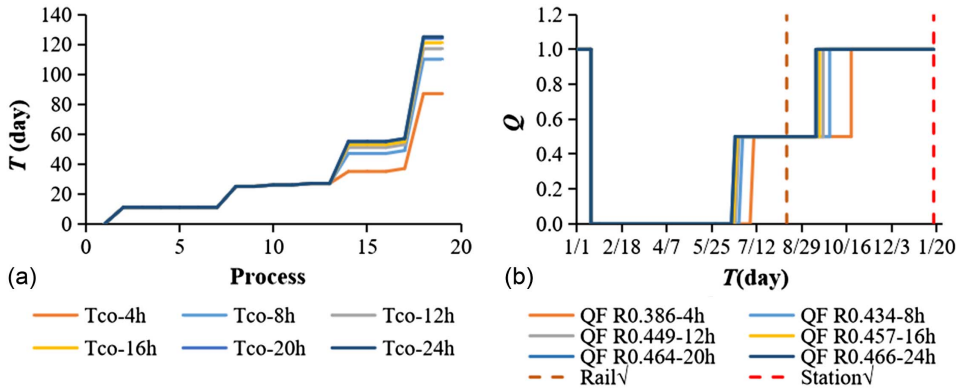

Fig. 12. Process-optimization time in China local restoration: (a) T-process of PAT restoration; and (b) Q_F-T of PAT restoration. Tco-4h represents the cumulative optimization time for 4 h of the average daily construction time scheme. QF R0.397-4h stands for the functional performance of the aforementioned scheme, and the functional resilience evaluation is 0.397.

Nat. Hazards Rev., 2023, 24(3): 04023019

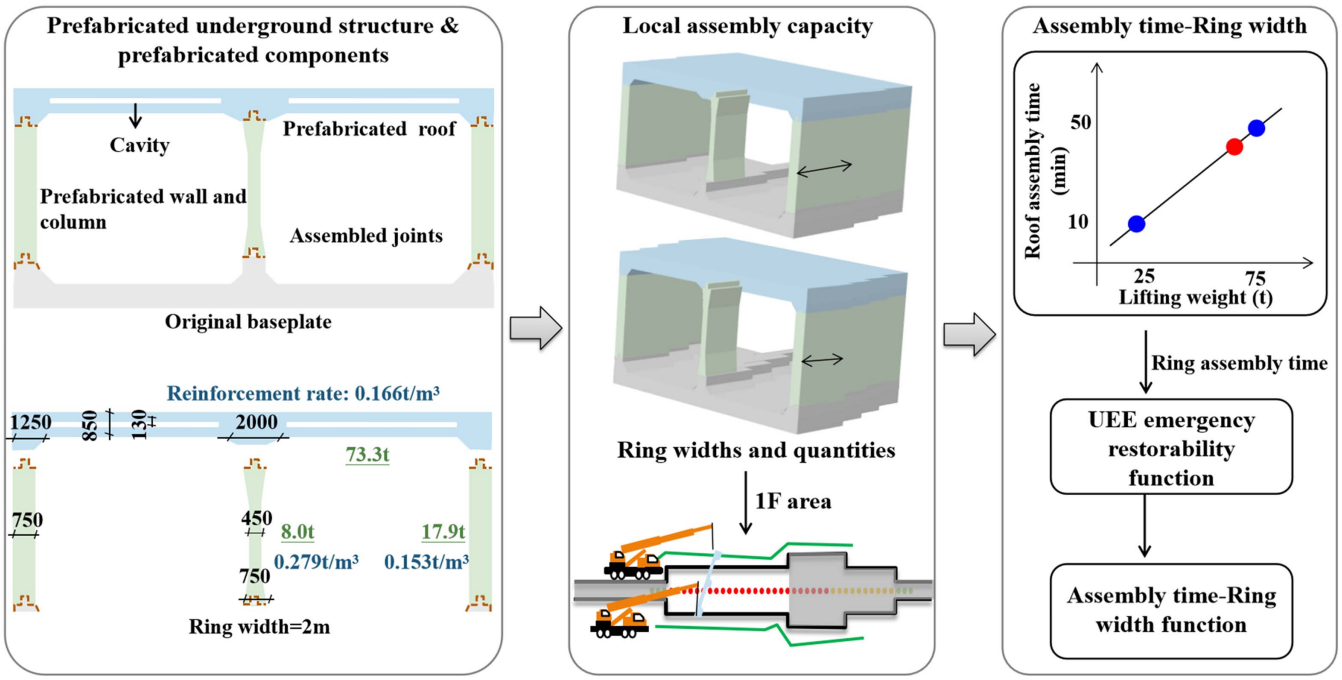

Fig. 13. Prefabricated underground structure inputs for local assembly capability adaptability analysis.

height cavity to reduce the weight by 10% and facilitate assembly construction. The weights of the 2-m-wide prefabricated roof, walls and 1.35-m-wide center column were calculated to be 73.3, 17.9, and 8.0 t, respectively (Fig. 13). The prefabricated component weights satisfied the aforementioned local assembly capacity requirements.

To analyze the prefabricated ring width and quantity adapted to the local assembly capacity, this study conducted an adaptability analysis for different local assembly capacities (Fig. 14). The representative 75-t assembly time was considered as the local assembly capacity (25-t assembly time was locked at 10 min). A range of 50 to 350 min was selected as the variable, with higher capacities taking shorter times. Initially, a linear relationship between assembly speed and lifting weight was determined, with 75- and 25-t assembly speeds as the two points. In this case, interpolating the assembly time of roofs with different ring widths was possible. The prefabricated single-ring assembly speed was calculated by substituting Eq. (1). Taking the 1F area as a case, the PAT emergency restorability, and assembly time were evaluated.

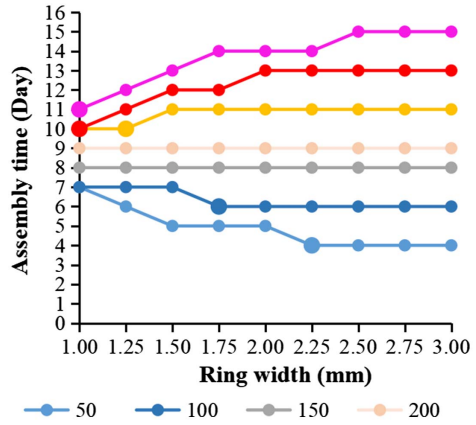

Fig. 14. Assembly time-ring width of different assembly capacities.

Assembly time-ring width functions with different assembly capacities were compared and analyzed. The results clearly present three types of characteristics: (1) for assembly speeds higher than 150 min/75 t, the assembly time decreased with increasing ring width; (2) for assembly speed between 150–200 min/75 t, the assembly time was insensitive to ring width; and (3) the assembly time decreased with decreasing ring width for assembly speeds lower than 200 min/75 t. This reveals the comprehensive performance of the three types of local assembly capabilities in PAT emergency restorability. When the local assembly capability is strong, the emergency restorability is sensitive to the prefabricated underground structure ring quantity, and the fewer rings are desired; conversely, the emergency restorability is sensitive to the ring weight, and lighter rings are preferred; the insensitive area is determined according to the UEE project requirements.

Based on local assembly capacity characteristics, adaptive schemes coordinated with the prefabricated underground structure and assembly capacity were explored. For the ring quantity sensitive assembly capacity, the minimum ring width of the lowest assembly time was chosen as the lower threshold. For the ring weight-sensitive assembly capacity, the maximum ring width at the lowest assembly time was chosen as the upper threshold, such as the largest dot of the curve in Fig. 14. The insensitive assembly capacity scheme was determined based on UEE project requirements. The assembly ring width threshold guided the design of the prefabricated underground structures. Adaptive schemes have a significant optimization effect. For example, a local assembly speed of 350 min/75 t can be optimized to a maximum of 4 days. Furthermore, it reduced the gap of assembly time from 11 to 7 days compared with a local assembly speed of 50 min/75 t. The adaptive schemes make full use of their respective effectiveness in emergency restorability, based on the local assembly capacity characteristics.

Discussion and Research Trends

This study constructed UEE emergency restorability functions for the comparative evaluation of local PAT and CIS restoration

schemes. We analyzed the optimization characteristics of emergency restorability incorporating the prefabricated underground structure and PAT technology. Finally, quantitative threshold and adaptability analyses of the local assembly capacities were performed. The methodology and results of this study are discussed as follows.

First, UEE emergency restorability has not been quantitatively assessed previously owing to the complex coupled disaster effect. The first function was proposed to establish the correlation between environmental restoration and structural restoration processes of UEE. The UEE emergency restorability provides an effective and rapid assessment of the performance-time-resilience of UEE restoration. The results provide a quantitative assessment of the post-disaster UEE resilience.

This study considered the application of PAT to UEE emergency restorability. First, the optimization effect of PAT restoration was quantitatively evaluated by comparing with CIS restoration. Second, the case study analysis revealed that the PAT restoration has a great potential for UEE resilience enhancement. Finally, after the adaptability analysis of the local assembly capacity, the local capacity can be maximized in the implementation of PAT restoration.

Second, the Q-T function indicated that the station's structural performance had a considerable stagnation period. The results indicated that UEE restoration involved numerous surrounding environmental works prior to station restoration. Therefore, the preliminary rail opening is extremely sensitive to the restoration of the surrounding environment. This study adopted meticulous subregions for microdisturbance and protection of the restoration of the surrounding environment. The efficiency of this measure in advancing the rail opening time was evident from the analysis results.

This inspired the study of the comprehensive resilience of the UEE. This study innovatively proposed the concept of an environment centered on an underground engineering. From the aforementioned research results, the UEE emergency restorability demands consideration of the individual and overall resilience performance of upper underground structures and the environment. A UEE emergency restoration function was constructed to evaluate the restoration project quantitatively. The restorability assessment of UEE facilitates an comprehensive resilience study with joint consideration of underground space and urban environment.

Third, the assembled structure is highly adaptable to emergency restoration. Traditional CIS restoration consumes significant environmental restoration and concrete engineering time. In contrast, PAT restoration achieves rapid UEE restoration through subregion and technical optimization. In particular, the application of PAT leads to the highest efficiency of technical optimization, indicating a significant advantage of this technology for UEE emergency restoration.

This inspired the combination of PAT to explore and improve the UEE emergency restorability. Unlike new construction, UEE restoration technology involves a series of complex and time-consuming measures. Integrating prefabricated underground structures and PAT can propose more efficient underground engineering restoration techniques. This has stimulated research to enhance UEE restoration strategies.

Fourth, PAT restoration depends on local assembly capacity. The analysis results indicated that the local assembly capacity must reach a minimum threshold to perform PAT restoration effectively. In addition, the UEE emergency restorability function provides precise control of local resources through the upper threshold for construction speed. In addition, we conducted a synergistic analysis of the prefabricated underground structure and local assembly capacity. An integrated design-construction" analysis method was developed to facilitate adaptation of emergency restorability to local assembly capacity.

This inspired the research on local assembly capacity. Because local assembly capacity is a cross-disciplinary study, it involves not only the technical level but also local social factors (He and Shi 2022). This facilitates the development of locally appropriate, fast, and efficient UEE restoration strategies that incorporate local factors.

Conclusion

This study developed a novel UEE emergency restorability function and PAT restoration scheme. First, the restoration levels were classified based on UEE damage patterns. Second, subregion and technical optimizations were performed to construct CIS/PAT restoration schemes. Third, CIS/PAT UEE emergency restorability functions were constructed. Finally, the performance of the CIS/PAT restoration, optimization effect, and local assembly capacities were analyzed using Daikai Station as a case study. The main conclusions are as follows:

- Meticulous subregion optimization reduced a large amount of environmental work. After this optimization, the environmental and structural work were only 0.56 and 0.71 of the CIS restoration. The subregion accumulative optimization time reached 27 days (13.5% speedup). Thus, this study advocates a protection and microdisturbance strategy for the surrounding environment rather than major restoration.
- Technical optimization incorporating PAT technology achieved rapid restoration. The technical optimization time reached 60.27% of the cumulative optimization time even at the lower threshold of the local assembly capacity. Therefore, this is the most efficient method for improving UEE emergency restorability.
- The structural and functional performance resilience of the PAT restoration was improved by 28.34% and 62.27%, respectively, compared with the CIS restoration. The results revealed the low efficiency of CIS restoration. In comparison, after two optimization efforts, PAT restoration had a higher potential for resilience improvement in urban transportation.
- Upper and lower thresholds were calculated for local assembly capacity. Setting lower and upper thresholds is necessary for PAT emergency restorability to function and refine emergency restoration resources. In this case, the upper and lower thresholds of assembly speed were 4.2 and 1.1 rings/day.
- The adaptability analysis revealed the performances of three local assembly capability types in PAT emergency restorability: ring quantity-sensitive, ring weight-sensitive, and insensitive.
- The adaptive scheme solved the competition between the local assembly speed and lifting weight and maximized the efficiency of different local assembly capacities in PAT restoration. After the adaptability analysis, the schemes with a high local assembly capacity reduced the assembly time, and the schemes with a poor local assembly capacity narrowed the gap with the large ones.

This study promotes a resilience study of an underground engineering from an individual entity to an environmental system. The UEE emergency restorability function is a quantitative assessment tool for urban resilience. PAT restoration schemes that integrate modern prefabrication technologies and local assembly capabilities provide strategies for resilience enhancement.

Data Availability Statement

All data, models, or code that support the findings of this study are available from the corresponding author upon reasonable request.

Acknowledgments

This study was supported by the National Natural Science Foundation of China (NSFC) (Project No. 52090084).

References

An, X., A. A. Shawky, and K. Maekawaa. 1997. "The collapse mechanism of a subway station during the Great Hanshin earthquake." *Cem. Concr. Compos.* 19 (3): 241–257. https://doi.org/10.1016/S0958-9465(97)00014-0.

Borri, A., M. Corradi, G. Castori, and A. Molinari. 2019. "Stainless steel strip—A proposed shear reinforcement for masonry wall panels." *Constr. Build. Mater.* 211 (Jun): 594–604. https://doi.org/10.1016/j.conbuildmat.2019.03.197.

Cao, L., Q. Fang, D. Zhang, and T. Chen. 2018. "Subway station construction using combined shield and shallow tunnelling method: Case study of Gaojiayuan Station in Beijing." *Tunnelling Underground Space Technol.* 82 (Dec): 627–635. https://doi.org/10.1016/j.tust.2018.09.010.

Chang, C.-T., C.-W. Sun, S. W. Duann, and R. Hwang. 2001. "Response of a Taipei Rapid Transit System (TRTS) tunnel to adjacent excavation." *Tunnelling Underground Space Technol.* 16 (3): 151–158. https://doi.org/10.1016/S0886-7798(01)00049-9.

Chen, Y., J. Lei, J. Li, Z. Zhang, Z. Yu, and C. Du. 2022. "Design characteristics on the indoor and outdoor air environments of the COVID-19 emergency hospital." *J. Build. Eng.* 45 (Jan): 103246. https://doi.org/10.1016/j.jobe.2021.103246.

Chinacrane.net. 2012. "Lifting of the world's largest dome for construction of the Second Bureau of China Construction has been successfully completed." [In Chinese.] Accessed September 14, 2012. http://www.chinacrane.net/news/201209/14/57190.html.

Civil Engineering Department. 1997. "Damage and restoration records to Daikai Subway station of Kobe rapid transit railway east and west line." [In Japanese.] Accessed January 1, 1997. http://www.lib.kobe-u.ac.jp/directory/eqb/book/11-276/html/pdf/3-2-0.pdf.

Ding, P., L. Tao, X. Yang, J. Zhao, and C. Shi. 2019. "Three-dimensional dynamic response analysis of a single-ring structure in a prefabricated subway station." *Sustainable Cities Soc.* 45 (Feb): 271–286. https://doi.org/10.1016/j.scs.2018.11.010.

Feng, Y. 2014. "Existing railroad shed hole construction technology: The application of truck crane lifting shed hole T-beam construction." [In Chinese.] *Sci. Technol. Vision* 17 (4): 119–121. https://doi.org/10.19694/j.cnki.issn2095-2457.2014.17.082.

He, J., and X. Shi. 2022. "Detection of social-ecological drivers and impact thresholds of ecological degradation and ecological restoration in the last three decades." *J. Environ. Manage.* 318 (Sep): 115513. https://doi.org/10.1016/j.jenvman.2022.115513.

Huang, H., D. Zhang, and Z. Huang. 2022. "Resilience of city underground infrastructure under multi-hazards impact: From structural level to network level." *Resilient Cities Struct.* 1 (2): 76–86. https://doi.org/10.1016/j.rcns.2022.07.003.

Joyner, M. D., M. H. Kurth, I. Pumo, and I. Linkov. 2021. "Recovery-based design of buildings for seismic resilience." *Int. J. Disaster Risk Reduct.* 65 (Nov): 102556. https://doi.org/10.1016/j.ijdrr.2021.102556.

Kong, J., C. Zhang, and S. P. Simonovic. 2021. "Optimizing the resilience of interdependent infrastructures to regional natural hazards with combined improvement measures." *Reliab. Eng. Syst. Saf.* 210 (Jun): 107538. https://doi.org/10.1016/j.ress.2021.107538.

Li, F., X. Du, and M. Zhang. 2014. "Statistical analysis of accidents in metro construction." [In Chinese.] *Chin. J. Underground Space Eng.* 10 (2): 474–479.

Li, W., and Q. Chen. 2020. "Seismic damage evaluation of an entire underground subway system in dense urban areas by 3D FE simulation." *Tunnelling Underground Space Technol.* 99 (May): 103351. https://doi.org/10.1016/j.tust.2020.103351.

Liu, S.-C., F.-L. Peng, Y.-K. Qiao, and J.-B. Zhang. 2021a. "Evaluating disaster prevention benefits of underground space from the perspective of urban resilience." *Int. J. Disaster Risk Reduct.* 58 (May): 102206. https://doi.org/10.1016/j.ijdrr.2021.102206.

Liu, Y., Y. Yuan, J. Shen, and W. Gao. 2021b. "Emergency response facility location in transportation networks: A literature review." *J. Traffic Transp. Eng.* 8 (2): 153–169. https://doi.org/10.1016/j.jtte.2021.03.001.

Luo, J., W. Deng, and Y. Tang. 2014. "Truck crane lifting prefabricated beam technology and benefit analysis." [In Chinese.] *Hunan Commun. Sci. Technol.* 40 (2): 123–127. https://doi.org/10.3969/j.issn.1008-844X.2014.02.037.

Ma, C.-X., F.-L. Peng, Y.-K. Qiao, and H. Li. 2023. "Influential factors of spatial performance in metro-led urban underground public space: A case study in Shanghai." *Underground Space* 8 (Feb): 229–251. https://doi.org/10.1016/j.undsp.2022.03.001.

Ma, P., R. Xin, and J. Yao. 2021. "Assessment of failure mode and seismic performance of damaged masonry structures retrofitted with grout-injected ferrocement overlay reinforcement (GFOR)." *Constr. Build. Mater.* 305 (Oct): 124778. https://doi.org/10.1016/j.conbuildmat.2021.124778.

Makisha, N. 2016. "Restoration and renovation of waste water pumping stations in case of emergency." *Procedia Eng.* 165 (Jan): 1087–1091. https://doi.org/10.1016/j.proeng.2016.11.823.

Mitoulis, S. A., S. A. Argyroudis, M. Loli, and B. Imam. 2021. "Restoration models for quantifying flood resilience of bridges." *Eng. Struct.* 238 (Jul): 112180. https://doi.org/10.1016/j.engstruct.2021.112180.

Mohammed, A. A., A. C. Manalo, W. Ferdous, Y. Zhuge, P. V. Vijay, A. Q. Alkinani, and A. Fam. 2020. "State-of-the-art of prefabricated FRP composite jackets for structural repair." *Eng. Sci. Technol. Int. J.* 23 (5): 1244–1258. https://doi.org/10.1016/j.jestch.2020.02.006.

Nakamura, S., J. Ezaki, I. Suetomi, N. Yoshida, and M. Iwafuji. 1997. "Investigation, analysis and restoration of the collapsed Daikai subway station during the 1995 Hyogoken Nambu earthquake." In *Proc., Paper Presented at the 3rd Kansai Int. Geotechnical Forum*. Tokyo: Civil engineering Dept.

Ouyang, M., and Z. Wang. 2015. "Resilience assessment of interdependent infrastructure systems: With a focus on joint restoration modeling and analysis." *Reliab. Eng. Syst. Saf.* 141 (Sep): 74–82. https://doi.org/10.1016/j.ress.2015.03.011.

Preciado, A., J. C. Santos, C. Silva, A. Ramírez-Gaytán, and J. M. Falcon. 2020. "Seismic damage and retrofitting identification in unreinforced masonry churches and bell towers by the September 19, 2017 (Mw = 7.1) Puebla-Morelos earthquake." *Eng. Fail. Anal.* 118 (Dec): 104924. https://doi.org/10.1016/j.engfailanal.2020.104924.

Ren, X., Z. Qiang, H. Dazhu, and B. Dengshan. 2021. "Seismic performance study on critically damaged masonry piers retrofitted using shear-compressive metal dampers." *Structures* 34 (Dec): 3906–3914. https://doi.org/10.1016/j.istruc.2021.10.022.

Sankei Shimbun. 1995. "Kobe expressway is ready for opening on the 13th." [In Japanese.] Accessed August 10, 1995. http://www.lib.kobe-u.ac.jp/directory/eqb/book/11-276/html/pdf/729(4_4_35).pdf.

Shabana, I., A. S. Farghaly, and B. Benmokrane. 2021. "Earthquake response of GFRP-reinforced concrete squat walls with aspect ratios of 1.14 and 0.68." *Eng. Struct.* 252 (Feb): 113556. https://doi.org/10.1016/j.engstruct.2021.113556.

Shi, P., and P. Li. 2015. "Mechanism of soft ground tunnel defect generation and functional degradation." *Tunnelling Underground Space Technol.* 50 (Aug): 334–344. https://doi.org/10.1016/j.tust.2015.08.002.

SOHU.com. 2018. "220 ton nuclear infrastructure dome lifting accuracy to millimeter! China Construction Second Engineering Bureau crowned Hualong 1." [In Chinese.] Accessed May 25, 2018. https://www.sohu.com/a/232903732_100095947.

Sthapit, N., and N. Sthapit. 2021. "Retrofitting of an RC frame building damaged in 'April 2015 Gorkha earthquake' in Kathmandu valley." *Prog. Disaster Sci.* 11 (Oct): 100192. https://doi.org/10.1016/j.pdisas.2021.100192.

Sun, C., 2020. "Construction process of pedestrian bridge steel structure lifting under complex environment." [In Chinese.] *City House* 27 (4): 210–211.

Sun, J., and Z. Zhang. 2020. "A post-disaster resource allocation framework for improving resilience of interdependent infrastructure networks."

Transp. Res. Part D: Transp. Environ. 85 (Aug): 102455. https://doi.org/10.1016/j.trd.2020.102455.

Tao, L., P. Ding, C. Shi, X. Wu, S. Wu, and S. Li. 2019. "Shaking table test on seismic response characteristics of prefabricated subway station structure." *Tunnelling Underground Space Technol.* 91 (Sep): 102994. https://doi.org/10.1016/j.tust.2019.102994.

Tencent. 2021. "The first fully prefabricated and assembled underground station in China has begun assembly, and these cities are also building PUS by building blocks." [In Chinese.] Accessed November 3, 2021. https://xw.qq.com/amphtml/20211103A08TYG00.

Tomar, A., and H. V. Burton. 2021. "Risk-based assessment of the post-earthquake functional disruption and restoration of distributed infrastructure systems." *Int. J. Disaster Risk Reduct.* 52 (Jan): 102002. https://doi.org/10.1016/j.ijdrr.2020.102002.

Xiang, N., X. Chen, and M. S. Alam. 2020. "Probabilistic seismic fragility and loss analysis of concrete bridge piers with superelastic shape memory alloy-steel coupled reinforcing bars." *Eng. Struct.* 207 (Mar): 110229. https://doi.org/10.1016/j.engstruct.2020.110229.

Xu, C.-X., S. Peng, J. Deng, and C. Wan. 2018. "Study on seismic behavior of encased steel jacket-strengthened earthquake-damaged composite steel-concrete columns." *J. Build. Eng.* 17 (May): 154–166. https://doi.org/10.1016/j.jobe.2018.02.010.

Yang, X., and F. Lin. 2021. "Prefabrication technology for underground metro station structure." *Tunnelling Underground Space Technol.* 108 (Feb): 103717. https://doi.org/10.1016/j.tust.2020.103717.

Yu, H., Y. Peng, L. Zhang, R. Wang, and Q. Wang. 2019. "Statistical analysis on urban metro accidents during construction period." [In Chinese.] Supplement, *Chin. J. Underground Space Eng.* 15 (S2): 852–860.

Yuan, W., S. Wang, H. Li, J. He, and X. Dang. 2021. "Development of intelligence and resilience for bridge seismic design." [In Chinese.] *China J. Highway Transp.* 34 (2): 98–117. https://doi.org/10.3969/j.issn.1001-7372.2021.02.003.

Zhang, C., J.-J. Kong, and S. P. Simonovic. 2018. "Restoration resource allocation model for enhancing resilience of interdependent infrastructure systems." *Saf. Sci.* 102 (Feb): 169–177. https://doi.org/10.1016/j.ssci.2017.10.014.

Zhang, C., C. Zhang, Q. Guo, B. Geng, and K. Hu. 2020. "Study on breakwater damage and emergency restoration under the influence of Typhoon Mangkhut." [In Chinese.] *China Harbour Eng.* 40 (8): 29–32.

Zhang, J.-L., X. Liu, J.-B. Zhao, Y. Yuan, and H. Mang. 2021. "Application of a combined precast and in-situ-cast construction method for large-span underground vaults." *Tunnelling Underground Space Technol.* 111 (May): 103795. https://doi.org/10.1016/j.tust.2020.103795.

Zhou, C., T. Kong, S. Jiang, S. Chen, Y. Zhou, and L. Ding. 2020. "Quantifying the evolution of settlement risk for surrounding environments in underground construction via complex network analysis." *Tunnelling Underground Space Technol.* 103 (Sep): 103490. https://doi.org/10.1016/j.tust.2020.103490.

Zhou, Y., H. Shao, Y. Cao, and E. M. Lui. 2021. "Application of buckling-restrained braces to earthquake-resistant design of buildings: A review." *Eng. Struct.* 246 (Nov): 112991. https://doi.org/10.1016/j.engstruct.2021.112991.

Zorn, C. R., and A. Y. Shamseldin. 2015. "Post-disaster infrastructure restoration: A comparison of events for future planning." *Int. J. Disaster Risk Reduct.* 13 (Sep): 158–166. https://doi.org/10.1016/j.ijdrr.2015.04.004.